

# $\Lambda$ effect in the cosmological expansion of voids

H.H. Fliche<sup>1</sup> and R. Triay<sup>2</sup>

<sup>1)</sup> LMMT\*, Fac. des Sciences et Techniques de St Jérôme  
av. Normandie-Niemen, 13397 Marseille Cedex 20, France

<sup>2)</sup> Centre de Physique Théorique <sup>†</sup>  
CNRS Luminy Case 907, 13288 Marseille Cedex 9, France  
e-mail: triay@cpt.univ-mrs.fr

December 2, 2024

## Abstract

The dynamical effect of the cosmological constant  $\Lambda$  on a single spherical void evolving in a Friedmann-Lemaître universe is investigated within a non linear perturbation of Newton-Friedmann models. The void expansion shows a huge initial burst, which freezes asymptotically up to match Hubble expansion.  $\Lambda$ -effect on the kinematics intervenes significantly by amplifying the expansion rate at redshift  $z \sim 1.7$ , what corresponds to the loitering period. As a result, the size increases with  $\Lambda$  (what can be interpreted by the “repulsion gravitational of vacuum”). A stability criterion is ensured for spatially closed Friedmann models, since the empty regions are swept out.

Keywords: Cosmology : Theory, Cosmological Constant, Voids, Large Scale Structures.

PACS: 98.80.-k, 98.65.Dx

## 1 Introduction

The understanding of the foam like patterns with large empty regions in the distribution of galaxies within scale up to 100 Mpc, which have been observed since three decades (see *e.g.*, [24, 13, 14, 6, 22, 4, 12, 3]), has become

---

\*UPRES EA 2596

<sup>†</sup>Unité Mixte de Recherche (UMR 6207) du CNRS, et des universités Aix-Marseille I, Aix-Marseille II et du Sud Toulon-Var. Laboratoire affilié à la FRUMAM (FR 2291).

an important challenge for the large scale formation theory. Such an investigation has been performed on their statistical properties by improving identification techniques (see *e.g.*, [21]), by exploring their formation process in a  $\Lambda$ CDM model through N-body simulations (see *e.g.*, [10, 23, 9, 17, 2, 26, 20]), by probing their origins (see *e.g.*, [19]), and on the kinematics of giant voids (see *e.g.*, [15]) and the dynamics by testing models of void formation (see *e.g.*, [8, 1]). Herein we contribute to such a goal by providing an exact solution of void dynamics. Thanks to their stability with respect to linear perturbations [16], Friedmann-Lemaître models provide us with a suitable description of the universe at large scales. These models can be described within a Newtonian approach (see *e.g.* [18]) by means of Euler-Poisson equations system solutions for whom kinematics satisfy Hubble (cosmological) law. Except the description of the gravitationnelles waves, Newtonian treatment of perturbations leads indeed to same results as those obtained in general relativity [7]. Herein, we define a model describing the dynamics of an empty spherical shell evolving in an expanding distribution of dust with the aim of understanding the effect of the cosmological constant on the evolution of the void.

## 2 Euler-Poisson equations system

The motion of a pressureless medium (dust) is described by its specific density  $\rho = \rho(\vec{r}, t)$  and velocity  $\vec{v} = \vec{v}(\vec{r}, t)$  at position  $\vec{r}$  and time  $t$ . These fields are constraint by Euler equations system

$$\frac{\partial \rho}{\partial t} + \text{div}(\rho \vec{v}) = 0 \quad (1)$$

$$\frac{\partial \vec{v}}{\partial t} + \frac{\partial \vec{v}}{\partial \vec{r}} \vec{v} = \vec{g} \quad (2)$$

where  $\vec{g} = \vec{g}(\vec{r}, t)$  stands for the gravitational field, and satisfy the modified Poisson-Newton equations

$$\overrightarrow{\text{rot}} \vec{g} = \vec{0} \quad (3)$$

$$\text{div} \vec{g} = -4\pi G \rho + \Lambda \quad (4)$$

where  $G$  is Newton constant of gravitation and  $\Lambda$  the cosmological constant.

For the purpose of our investigation, it is convenient to write these equations with new coordinates, herein named *reference coordinates*, defined by

$$(t, \quad \vec{x} = \frac{\vec{r}}{a}), \quad a > 0 \quad (5)$$

where  $a = a(t)$  is a monotonic function which verifies Friedmann equation

$$\dot{H} + H^2 - \frac{\Lambda}{3} + \frac{4\pi G}{3}\rho_{\circ}a^{-3} = 0, \quad H = \frac{\dot{a}}{a}, \quad a_{\circ} = 1 \quad (6)$$

where  $\rho_{\circ}$  is an arbitrary constant, the dotted variables stand for time derivatives. This differential equation admits an integration constant

$$K_{\circ} = \frac{8\pi G}{3}\rho_{\circ} + \frac{\Lambda}{3} - H_{\circ}^2 \quad (7)$$

and hence integrates for providing us with

$$H^2 = \frac{\Lambda}{3} - \frac{K_{\circ}}{a^2} + \frac{8\pi G}{3}\frac{\rho_{\circ}}{a^3} \geq 0 \quad (8)$$

The function  $H(a)$  shows an asymptotical value

$$H_{\infty} = \lim_{a \rightarrow \infty} H = \sqrt{\frac{\Lambda}{3}} \quad (9)$$

and provides us with  $t \mapsto a$  (as reciprocal mapping of a quadrature). Thus the function  $a(t)$  depends on three parameters chosen among  $\Lambda$ ,  $\rho_{\circ}$ ,  $H_{\circ}$  and  $K_{\circ}$ , see Eq. (7).

Let  $\overrightarrow{\text{div}}$  and  $\overrightarrow{\text{rot}}$  denote the differential operators defined with respect to  $\vec{x}$ , Euler-Poisson-Newton equations system reads in term of reference coordinates defined in Eq. (5) as follows

$$\frac{\partial \rho_c}{\partial t} + \text{div}(\rho_c \vec{v}_c) = 0 \quad (10)$$

$$\frac{\partial \vec{v}_c}{\partial t} + \frac{\partial \vec{v}_c}{\partial \vec{x}} + 2H\vec{v}_c = \vec{g}_c \quad (11)$$

$$\overrightarrow{\text{rot}} \vec{g}_c = \vec{0} \quad (12)$$

$$\text{div} \vec{g}_c = -\frac{4\pi G}{a^3}(\rho_c - \rho_{\circ}) \quad (13)$$

where

$$\rho_c = \rho a^3, \quad \vec{v}_c = \frac{d\vec{x}}{dt} \quad (14)$$

act respectively as the density and the velocity fields of medium in the *reference frame*, and

$$\vec{g}_c = \frac{\vec{g}}{a} + \left( \frac{4\pi G}{3a^3}\rho_{\circ} - \frac{\Lambda}{3} \right) \vec{x} \quad (15)$$

as the acceleration field.

## 2.1 Newton-Friedmann and Void models

Equations (10, 11) have two obvious solutions :

1. herein named Newton-Friedmann model (NF), it is defined by

$$\rho_c = \rho_o, \quad \vec{v}_c = \vec{0}, \quad \vec{g}_c = \vec{0} \quad (16)$$

According to Eq.(8,14),  $a$  and  $H$  recover now their usual interpretations in cosmology as *expansion parameter* and *Hubble parameter* respectively,  $\rho_o = \rho a^3$  identifies to the density of sources in the co-moving space and  $K_o$  (interprets in General Relativity as) its scalar curvature. We limit our investigation to motions which do not correspond to bouncing solutions. Accordingly, an analysis on roots of third degree polynomials tell us that the constraint

$$K_o^3 < (4\pi G \rho_o)^2 \Lambda \quad (17)$$

must be satisfied. Hence, the kinematics shows two distinct behaviours, which are characterised by the sign of  $K_o$  :

- if  $K_o > 0$  then  $H$  decreases with  $a$  down to a minimum defined by

$$H_m = H_\infty \sqrt{1 - \frac{K_o^3}{\Lambda (4\pi G \rho_o)^2}} \quad (18)$$

at  $a = 4\pi G \rho_o K_o^{-1}$  and hence it increases toward its asymptotic value  $H_\infty$  as defined in Eq.(9).

- if  $K_o \leq 0$  then  $H$  decreases with  $a$  down to  $H_\infty$ .

2. herein named Void model (V), it is defined by

$$\rho_c = 0, \quad \vec{v}_c = (H_\infty - H) \vec{x}, \quad \vec{g}_c = \frac{4\pi G}{a^3} \rho_o \vec{x} \quad (19)$$

## 3 Spherical voids in Newton-Friedman universe

For modelling the dynamics of a spherical void in a uniform dust distribution we use a covariant formulation of Euler-Poisson equations system (see Appendix A). The model, which is obtained by sticking together the local solutions V and NF of Euler-Poisson equations system as given in Sec. (2.1), accounts for the dynamics of boundaries conditions. It describes the evolution of their common border, which is a *material shell*, see Sec. 3.1. For

conveniences in writing, each symbol S, V and NF denotes both the medium and the related dynamical model respectively. A qualitative analysis of solutions is performed in Sec. (3.2) with respect of model parameters and in particular the cosmological constant  $\Lambda$ .

### 3.1 Dynamical model of spherical voids

We consider three distinct media : a material shell (S), an empty inside (V) and a uniform dust distribution outside (NF). These media behave such that S makes the juncture of V with NF as given in Eq. (16,19). The tension-stress on S is assumed to be negligible, which is characterised by a (symmetric contravariant) mass-momentum tensor defined as follows

$$T_S^{00} = (\rho_S)_c, \quad T_S^{0j} = (\rho_S)_c v_c^j, \quad T_S^{jk} = (\rho_S)_c v_c^j v_c^k \quad (20)$$

and outside S, the mass-momentum tensor of NF reads

$$T_{NF}^{00} = \rho_c, \quad T_{NF}^{0j} = 0, \quad T_{NF}^{jk} = 0 \quad (21)$$

Since the eulerian function(al)

$$\mathcal{T}(x \mapsto \gamma) = \int T_S^{\mu\nu} \gamma_{\mu\nu} dt dS + \int T_{NF}^{\mu\nu} \gamma_{\mu\nu} dt dV \quad (22)$$

vanishes when  $\gamma$  reads in the form  $\gamma_{\mu\nu} = \frac{1}{2} (\hat{\partial}_\mu \xi_\nu + \hat{\partial}_\nu \xi_\mu)$ , one has

$$\begin{aligned} & \int_S \left( (\partial_0 \xi_0 + g_c^j \xi_j) + (\partial_j \xi_0 + \partial_0 \xi_j - 2H \xi_j) v_c^j + v_c^j v_c^k \partial_j \xi_k \right) (\rho_S)_c dt x^2 d\Omega \\ &= - \int_{NF} \rho_c \partial_0 \xi_0 dt x^2 dx d\Omega \end{aligned} \quad (23)$$

where  $d\Omega$  stands for the solid angle element. The radial symmetry of solutions enables us to write the *reduced* peculiar velocity and acceleration of a test particle located on the shell as follows

$$\vec{v}_c = \alpha \vec{x}, \quad \vec{g}_c = \beta \vec{x} \quad (24)$$

where the functions  $\alpha = \alpha(t)$  and  $\beta = \beta(t)$  have to be determined. A by part integration of Eq. ( 23) provides us with

$$\begin{aligned} & \int_{t_1}^{t_2} (\partial_0 (\rho_S)_c + 3(\rho_S)_c \alpha - \rho_c \alpha x) x^2 \xi_0 dt \\ &= \int_{t_1}^{t_2} (\partial_0 ((\rho_S)_c \alpha) + 4(\rho_S)_c \alpha^2 + 2H(\rho_S)_c \alpha - (\rho_S)_c \beta x^{-1}) x^3 \tilde{\xi} dt \end{aligned} \quad (25)$$

where  $x = \|\vec{x}\|$  stands for the radius of S and  $\tilde{\xi} = \sqrt{\xi_1^2 + \xi_2^2 + \xi_3^2}$ . This equality must be fulfilled for all bounded time interval and compact support 1-form. Hence, we easily derive the conservation equations for the mass

$$\partial_0(\rho_S)_c + (3(\rho_S)_c - \rho_c x) \alpha = 0 \quad (26)$$

and for the momentum

$$\frac{d\alpha}{dt} + \left(1 + \frac{\rho_c}{(\rho_S)_c} x\right) \alpha^2 + 2H\alpha + \frac{\beta}{x} = 0 \quad (27)$$

With Eq. (5), the calculation of the gravitational force from the entire shell acting on a particular point<sup>1</sup> provides us with

$$\beta = \frac{4\pi G}{a^3} \left( \frac{\rho_c}{3} - \frac{(\rho_S)_c}{2x} \right) \quad (28)$$

About mass conservation, it is noticeable that

$$(\rho_S)_c = \frac{1}{3} \rho_c x \quad (29)$$

is solution of Eq. (26), what ensures that the amount of matter which forms the shell comes from its interior. Hence, Eq. (27) transforms

$$\frac{d\alpha}{dt} + 4\alpha^2 + 2H\alpha - \frac{2\pi G}{3} \frac{\rho_c}{a^3} = 0 \quad (30)$$

It is convenient to use the dimensionless variable

$$\chi = 4 \frac{\alpha}{H_o} a^2 \quad (31)$$

where the ratio  $\alpha H_o^{-1}$  stands for the expansion rate of S in the reference frame. Hence, Eq. (30) transforms into a Riccati equation

$$\frac{d\chi}{da} = \left( \Omega_o - \frac{\chi^2}{a} \right) \frac{1}{\sqrt{P(a)}} \quad (32)$$

where

$$P(a) = \lambda_o a^4 - k_o a^2 + \Omega_o a, \quad P(1) = 1 \quad (33)$$

with the following dimensionless parameters

$$\lambda_o = \frac{\Lambda}{3H_o^2}, \quad \Omega_o = \frac{8\pi G \rho_o}{3H_o^2}, \quad k_o = \frac{K_o}{H_o^2} \quad (34)$$

---

<sup>1</sup>The modified newtonian gravitation field reads  $\vec{g} = \left( \frac{\Lambda}{3} - \frac{Gm}{r^3} \right) \vec{r}$

Hence, according to Eq. (14,31), the radius of S is given by

$$x = x_i \exp \left( \int_{a_i}^a \frac{\chi da}{4a\sqrt{P(a)}} \right) \quad (35)$$

where  $x_i$  and  $a_i$  stands for the initial values at time  $t_i$ .

### 3.2 Qualitative analysis

For the analysis of the expansion of the shell S, we use the following dimensionless quantities : the *magnification*  $X$  and the *expansion rate*  $Y$ , which are defined as follows

$$X = \frac{x}{x_i}, \quad Y = \frac{\alpha}{H_o} \quad (36)$$

Their corresponding diagrams versus the expansion parameter  $a$  characterise the dynamics of S, they are obtained from Eq. (32, 35) by numerical integration. The evolution of  $X$  and  $Y$  with cosmic time  $t$  and/or with redshift  $z$  can be derived in a straightforward way, since the mapping  $t \mapsto a(t) = 1/(1+z)$  is a monotonic function of  $t$  in the present investigation. Instead of having an exhaustive analysis, we limit our investigation around the generally accepted values of cosmological parameters  $\lambda_o = 0.7$  and  $\Omega_o = 0.3$ . The initial conditions lie on the expansion rate  $Y_i$  and/at the formation date  $t_i$  of the void as expressed by means of  $a_i = a(t_i)$ . Similarly as for the previous cosmological parameters values, the values  $a_i = 0.003$  and  $Y_i = 0$  (void initially expanding with Hubble flow) are used as standard in our discussion. The kinematics of the expansion is described in Sec.3.2.1, the dependence on cosmological parameters is analysed in Sec. 3.2.2, and on initial conditions in Sec. 3.2.3. A synthesis of these results is given in Sec. 3.4.

#### 3.2.1 Kinematics

The expansion velocity of the shell S with respect to its centre reads

$$\vec{v} = yH\vec{r}, \quad y = 1 + \frac{Y}{h}, \quad h = \frac{H}{H_o} \quad (37)$$

where  $H_o$  stands for the value of Hubble parameter at time  $t_o$  (*i.e.*,  $a_o = a(t_o) = 1$ ) and  $y$  for the corrective factor to Hubble expansion. The general trend of the kinematics is given by the diagram  $y$  versus  $\ln a$  in Fig. 1. It results from the initial conditions  $a_i = 0.003$ ,  $Y_i = 0$ , and the cosmological parameters  $\Omega_o = 0.3$ . and  $\lambda_o = 0$ ,  $\lambda_o = 0.7$ ,  $\lambda_o = 1.4$ . The shell S expands faster than Hubble expansion ( $y > 1$ ) at early stages of its evolution with no

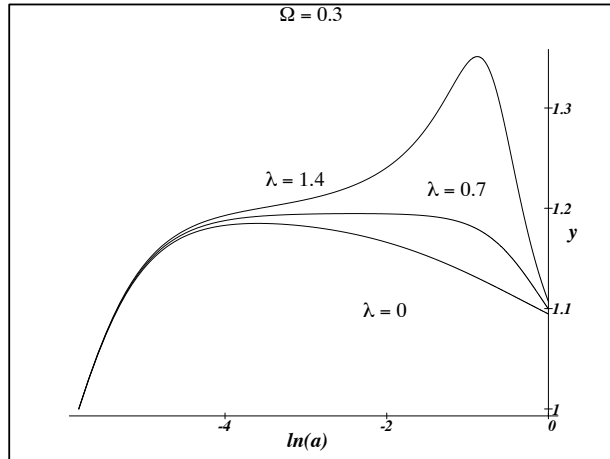


Figure 1: The corrective factor to Hubble expansion.

significant dependence on  $\Lambda$ , which appears later.  $\Lambda$ -effect is characterised by a significant protuberance at  $z \sim 1.7$  on the diagram, the larger the  $\lambda_0$  the higher the bump. It is due to the existence of a minimum value  $H_m$  of Hubble parameter  $H$  which is reached during the cosmological expansion (also referenced as a loitering period), see Eq.(18). After this period the kinematics reaches asymptotically Hubble expansion. It is interesting to note that the present epoch ( $a = 1$ ) seems to be quite peculiar because of the relative proximity of curves, but it is solely an artefact<sup>2</sup>.

### 3.2.2 Dependence on cosmological parameters

The growth of spherical voids is investigated by means of X and Y diagrams with respect of cosmological parameters  $\Omega_0$  and  $\lambda_0$ , with the aim of disentangling their related effects, herein named  $\Omega$ -effect and  $\Lambda$ -effect respectively.

1. The dependence on the outside density. — The comparison of diagrams with a vanishing cosmological constant  $\lambda_0 = 0$  corresponding to parameter values  $\Omega_0 = 0.15, 0.3, 0.45$  on Fig. 2 shows that the larger the  $\Omega_0$  the larger the magnification. Such an effect results from the attraction of shell particles toward denser regions. The growth looks

---

<sup>2</sup>Indeed, the three curves cross with  $a > 1$  but not in only one point.



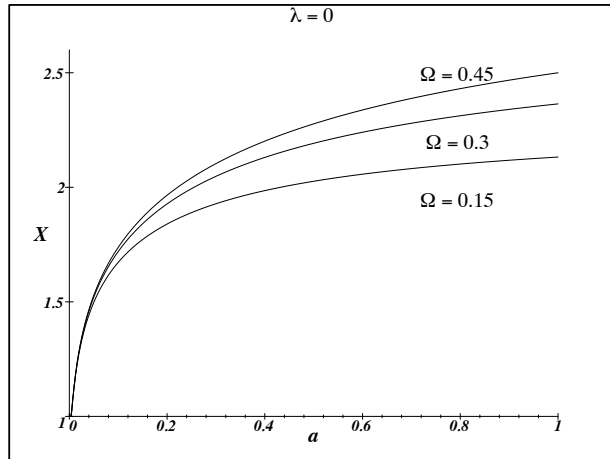


Figure 2: The magnification  $X$  — dependence on density.

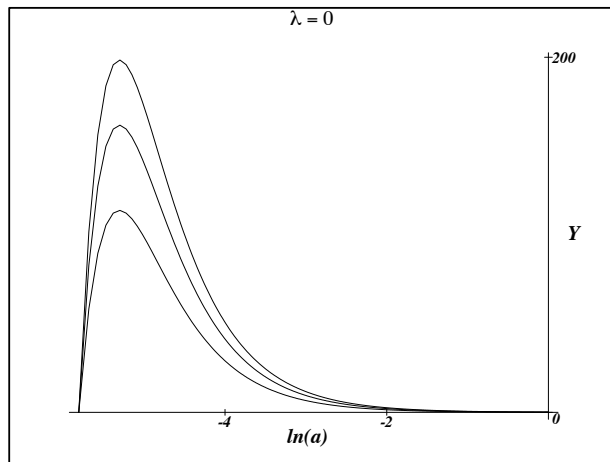


Figure 3: The expansion rate  $Y$  — dependence on density.

like a huge burst which freezes asymptotically up to matching Hubble expansion ( $Y = 0$ ), the larger the  $\Omega_o$  the larger the expansion rate  $Y$ , see Fig. 3. This trend is not significantly modified by another acceptable values of  $\lambda_o$ .

2. The dependence on the cosmological constant. — With a constant  $\Omega_o = 0.3$  the comparison of diagrams corresponding to parameter values  $\lambda_o = 0, 0.7, 1.4$  on Fig 4 shows that the larger the  $\lambda_o$  the larger the magnification. As for  $\Omega$ -effect,  $\Lambda$ -effect amplifies the magnifica-

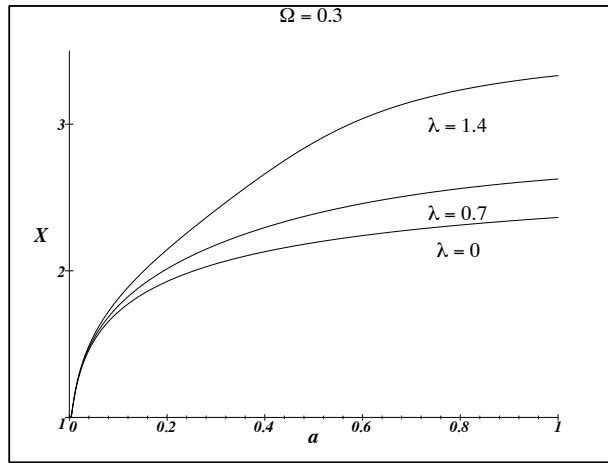


Figure 4: The magnification  $X$  — dependence on the cosmological constant.

tion which increases nonlinearly with  $\lambda_o$ . This phenomenon interprets as the “repulsive effect of vacuum” (if  $\Lambda > 0$ ). The expansion rate  $Y$  does not characterises  $\Lambda$  since the related curves do not disentangle, see Fig 5. Figure 1 shows that  $\Lambda$ -effect is late, and although not very significant on  $Y$  it has a cumulative effect which is reflected on magnification  $X$ .

3. Interpretation of parameter  $k_o$ . — A straightforward analysis of Eq. (19) shows that a test-particle moves from the inside toward the shell as long as  $H < H_\infty$ , what interprets as a stability criterion since the void is swept out. Such a criteria is fulfilled only if  $k_o > 0$ . A dimensional analysis of Eq. (7) shows that the Newtonian interpretation of  $k_o = \lambda_o + \Omega_o - 1$  corresponds to a dimensionless binding energy for

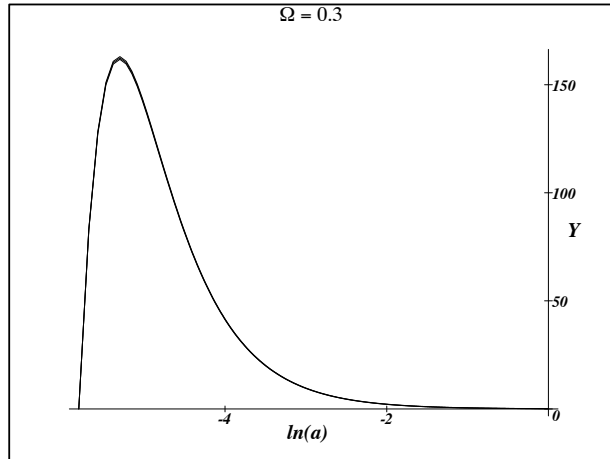


Figure 5: The expansion rate  $Y$  — dependence on the cosmological constant.

the universe<sup>3</sup>. This provides us with a meaningful procedure for comparing the magnitudes of  $\Lambda$ -effect or  $\Omega$ -effect between different world models at constant  $k_o$ . Let us remind that for Friedmann model  $k_o$  stands for the dimensionless spatial curvature (of the comoving space),  $k_o > 0$  correspond to spatially closed universes.

### 3.2.3 Dependence on the initial conditions

The dependence of  $S$  on the formation date is investigated with  $Y_i = 0$  and  $a_i = 0.003$ ,  $a_i = 0.03$ , and  $a_i = 0.3$  respectively, and by assuming  $\Omega_o = 0.3$  and  $\lambda_o = 0.7$ . According to Fig. 6, the earlier the date of birth the larger the magnification  $X$ . Figure 7 suggests the existence of a limiting curve  $a \mapsto Y$  defined by  $a_i = 0$ , which characterises  $\Omega_o$ . All expansion rate curves related to other formation dates are located in lower part and reach it asymptotically. One can expect that the effects on the dynamics of growth resulting from reasonable initial expansion rates  $Y_i \neq 0$ , related to physical processes (*e.g.*, supernovae explosions), are negligible at primordial epoch<sup>4</sup>,

<sup>3</sup>The lower  $k_o$  the faster the cosmological expansion. Note that it works with an opposite direction for the expansion of spherical voids.

<sup>4</sup>Since Hubble expansion is all the more important towards the past, the earlier the formation date the weaker this effect, according to Eq. (37).

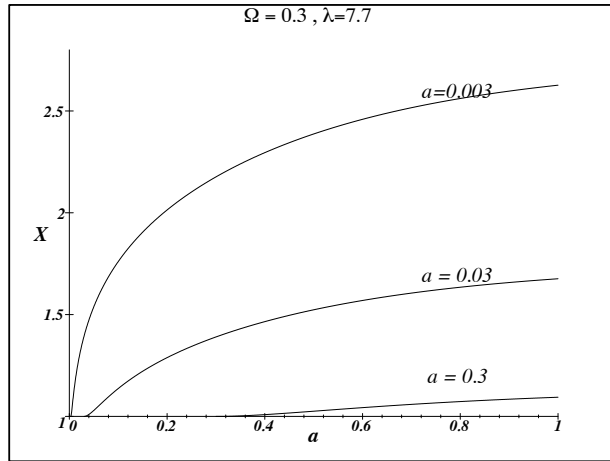


Figure 6: The magnification  $X$  — dependence on the formation date.

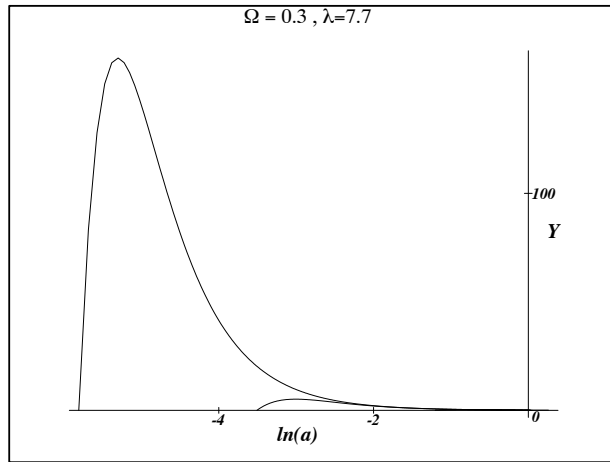


Figure 7: The expansion rate  $Y$  — dependence on the formation date.

what legitimises the initial condition  $Y_i = 0$  at  $a_i = 0.003$ . Evolutions with other initial conditions on  $Y_i$  can be deduced from that since any given point  $(a_i, Y_i)$  in the diagram belongs to a single evolution curve.

### 3.3 Synthesis

As a result, the expansion (in the reference frame) of spherical voids increases (non linearly) with the cosmological parameters  $\Omega_o$  and  $\lambda_o$ , what interprets respectively by the gravitational attraction from the outer parts and by the gravitational repulsion of vacuum from the inner parts. The larger these parameters the higher the magnification  $X$ . The dynamics is sensitive to  $\Omega$ -effect at primordial epochs and to  $\Lambda$ -effect later on. The evolution of the expansion rate  $Y$  with time does not characterise the cosmological constant  $\Lambda$  but the density parameter  $\Omega_o$ . The related diagram stands for an envelope curve which fits expansion rate evolutions related to other formation dates. On the other hand, the cosmological constant intervenes significantly on the kinematics by means of the corrective factor  $y$  to Hubble expansion, which shows a bump at a characteristic redshift  $z \sim 1.7$  (with  $\Omega_o = 0.3$ ), its amplitude increases with  $\Lambda$ . According to Eq. (37), the perturbation on redshift of sources located on the shell of expanding voids does not exceed

$$\Delta z = \frac{XY}{1+z} \frac{x_i H_o}{c} \quad (38)$$

which is a tiny value ( $\sim 10^{-3}$ ) because of counterbalancing behaviours of  $X$  and  $Y$ .

### 3.4 Discussion

Because Newtonian approach is used instead of general relativity, this model applies solely to reasonable sized voids<sup>5</sup> so that the main features should remain qualitatively reliable. Moreover, it is clear that such a model should be applied with caution to observed distribution of galaxies since the effects related to foamlike patterns are not considered. On the other hand, this model is based on the connection of two exact solutions of Euler-Poisson equations system, what is a huge advantage for investigating properly the behaviour of a single void and provides us with an appreciable hint to the dynamics.

---

<sup>5</sup>At first glance, one might argue that the related scale should be larger than the size of background structures in order to make the uniform density hypothesis an acceptable approximation, what looks like a dilemma. However, such an hypothesis, which applies to the entire universe, is ensured by the isotropy of CMB.

## 4 Conclusion

We investigate the dynamics of an isotropic universe constituted by a spherical void surrounded by a uniform distribution of dust by means of Euler-Poisson equations system with cosmological constant. It turns out that the behaviours of both regions (inside and outside the shell) coincide with Friedmann solutions. The connection conditions between these two regions are investigated in Classical Mechanics, what provides us with the dynamics of the shell. Let us emphasise that such a schema does not correspond to the usual embedding of a void solution into a cosmological background solution, but interprets as a non linear perturbation of Newton-Friedmann (NF) models.

The general behaviour of the void expansion shows a huge initial burst, which freezes asymptotically up to match Hubble expansion. While the corrective factor to Hubble law on the shell depends weakly on cosmological constant at early stages, it enables us to disentangle significantly cosmological models around redshift  $z \sim 1.7$ . The magnification of spherical voids increases with the density parameter and with the cosmological constant. An interesting feature is that for NF-models which correspond to spatially closed Friedmann models, the empty regions are swept out, what provides us with a stability criterion.

## A Appendix : Covariant formulation of Euler-Poisson equations system

Souriau's covariant formulation of Euler-Poisson equations[25] can be summarized as follows : The geometrical interpretation of Newton dynamics[5] shows that the component of gravitational field  $\vec{g}$  identify to the only non null Christoffel components of newtonian connexion

$$\Gamma_{00}^j = -g^j$$

Hence, one obtains their expression in the new coordinates system defined in Eq. (5), and the only non null components read

$$(\Gamma_c)^j_{k0} = H\delta_k^j, \quad (\Gamma_c)^j_{00} = -g_c^j$$

Let  $\mathcal{T}$  be a function(al) defined on the set of symmetric density tensors  $x \mapsto \gamma$  on newtonian spacetime  $\mathbb{R}^4$

$$\mathcal{T}(x \mapsto \gamma) = \int_{\mathbb{R}^4} T^{\mu\nu} \gamma_{\mu\nu} dt dV$$

where  $dtdV$  stands for the volume element and  $T$  for a symmetric contravariant tensors which accounts for the media. The measure density  $\mathcal{T}$  is eulerian if and only if it vanishes for all covariant tensor fields which reads

$$\gamma_{\mu\nu} = \frac{1}{2} \left( \hat{\partial}_\mu \xi_\nu + \hat{\partial}_\nu \xi_\mu \right)$$

where  $\hat{\partial}$  stands for the covariant derivative and  $x \mapsto \xi$  for a compact support 1-form. In such a case, it is obvious to show that

$$\hat{\partial}_\mu T^{\mu\nu} = 0$$

interprets as Euler equations, in any coordinates systems.

## References

- [1] K. Bolejko, *Mon. Not. R. Astron. Soc.* **370**, 924 (2006)
- [2] J.M. Colberg, in *Outskirts of Galaxy Clusters : intense life in the suburbs*, Proc. IAU Coll. **195**, 51 (2004) A. Diaferio, ed.
- [3] C. Conroy, A.L. Coil, M. White, J.A. Newman, R. Yan, M.C. Cooper, B.F. Gerke, M. Davis, D.C. Koo *Astrophys. J.* **635**, 990 (2005)
- [4] D.J. Croton, M. Colless, E. Gaztaaga, C.M. Baugh, P. Norberg, I. K. Baldry, J. Bland-Hawthorn, T. Bridges, R. Cannon, S. Cole, C. Collins, W. Couch, G. Dalton, R. De Propris, S. P. Driver, G. Efstathiou, R. S. Ellis, C. S. Frenk, K. Glazebrook, C. Jackson, O. Lahav, I. Lewis, S. Lumsden, S. Maddox, D. Madgwick, J. A. Peacock, B. A. Peterson, W. Sutherland, K. Taylor, The 2dFGRS team, *Mon. Not. R. Astron. Soc.* **352**, 828 (2004)
- [5] C. Duval, H.P. Künzle, *Rep. Math. Phys.* **13**, 351 (1978)
- [6] P.J. Einasto, in Proc. of Ninth Marcel Grossmann Meeting on General Relativity, p. 291 . Edits. V.G. Gurzadyan, R.T. Jantzen, Ser. Edit. R. Ruffini. World Scientific (2002)
- [7] H.H. Fliche, in *Évaluation des paramètres cosmologiques à l'aide des propriétés optiques des quasars. Fluctuations des modèles de Friedmann-Lemaître*, thèse d'état – Univ. de Provence (1981)
- [8] Y.Friedmann, T. Piran, *Astrophys. J.* **548**, 1 (2001)

- [9] D.M. Goldberg, M.S. Vogeley *Astrophys. J.* **605**, 1 (2004)
- [10] S. Gottlöber, E.L. Lokas, A. Klypin, Y. Hoffman, *Mon. Not. R. Astron. Soc.* **344**, 715 (2003)
- [11] V. Icke, *Mon. Not. R. Astron. Soc.* **206**, 1 (1984)
- [12] J. Jaaniste, M. Einasto, J. Einasto, *Astroph. Space Sci.* **290**, 187 (2004)
- [13] M. Joevee, J. Einasto, in *The Large Scale Structure of the Universe*. IAU Symp. **79**, 241. Eds. M.S. Longair & J. Einasto (1978)
- [14] R.P. Kirshner, A. Oemler, P.L. Shechter, S.A. Shechtman *Astrophys. J.* **248**, L57 (1981)
- [15] H. Mathis, J. Silk, L.M. Griffiths, M. Kunz, *Astron. Astrophys.* **382**, 389 (2002)
- [16] E.M. Lifchitz, I.M. Khalatnikov, *Usp. Fiz. Nauk.* **80**, 391 (1963); *Adv. Phys.* **12**, 185 (1963)
- [17] H. Mathis, J. Silk, L.M. Griffiths, M. Kunz, *Mon. Not. R. Astron. Soc.* **350**, 287 (2004)
- [18] W.H. Mc Crea, *Astron. J.* **60**, 271 (1955)
- [19] L.M. Ord, M. Kunz, H. Mathis, J. Silk, *Pub. Astron. Soc. Austr.* **22**, 2,166 (2005)
- [20] N.D. Padilla, L. Ceccarelli, D.G. Lambas, *Mon. Not. R. Astron. Soc.* **363**, 977 (2005)
- [21] S. G. Patiri, J. E. Betancort-Rijo, F. Prada, A. Klypin, S. Gottlöber, *Mon. Not. R. Astron. Soc.* **369**, 335 (2006)
- [22] R.R. Rojas, M.S. Vogeley, F. Hoyle, J. Brinkmann, *Astrophys. J.* **617**, 50 (2004)
- [23] S.F. Shandarin, J.V. Sheth, V. Sahni, *Mon. Not. R. Astron. Soc.* **353**, 162 (2004)
- [24] R.M. Soneira, P.J.E. Peebles, *Astron. J.* **83**, 845 (1978)



- [25] J.-M. Souriau, (French) C. R. Acad. Sci. Paris Sér. A , p. 751 (1970); (French) C. R. Acad. Sci. Paris Sér. A , p.1086 (1970); “Milieux continus de dimension 1, 2 ou 3 : statique et dynamique” in *Actes du 13ème Congrès Français de Mécanique*, AUM, Poitiers-Futuroscope, p.41 (1997)
- [26] R. van de Weygaert, R. Sheth, and E. Platen, in *Outskirts of Galaxy Clusters : intense life in the suburbs*, Proc. IAU Coll. **195**, 1 (2004) A. Diaferio, ed.